European Journal of Biophysics
2017; 5(1): 7-16
http://www.sciencepublishinggroup.com/j/ejb
doi: 10.11648/j.ejb.20170501.12
ISSN: 2329-1745 (Print); ISSN: 2329-1737 (Online)

Evaluation of Structural Properties and Isotopic Abundance Ratio of Biofield Energy Treated (The Trivedi Effect®) Magnesium Gluconate Using LC-MS and NMR

Mahendra Kumar Trivedi[1], Alice Branton[1], Dahryn Trivedi[1], Gopal Nayak[1], Alan Joseph Balmer[1], Dimitrius Anagnos[1], Janice Patricia Kinney[1], Joni Marie Holling[1], Joy Angevin Balmer[1], Lauree Ann Duprey-Reed[1], Vaibhav Rajan Parulkar[1], Parthasarathi Panda[2], Kalyan Kumar Sethi[2], Snehasis Jana[2, *]

[1]Trivedi Global, Inc., Henderson, Nevada, USA

[2]Trivedi Science Research Laboratory Pvt. Ltd., Bhopal, Madhya Pradesh, India

Email address:

publication@trivedieffect.com (S. Jana)

[*]Corresponding author

To cite this article:

Mahendra Kumar Trivedi, Alice Branton, Dahryn Trivedi, Gopal Nayak, Alan Joseph Balmer, Dimitrius Anagnos, Janice Patricia Kinney, Joni Marie Holling, Joy Angevin Balmer, Lauree Ann Duprey-Reed, Vaibhav Rajan Parulkar, Parthasarathi Panda, Kalyan Kumar Sethi, Snehasis Jana. Evaluation of Structural Properties and Isotopic Abundance Ratio of Biofield Energy Treated (The Trivedi Effect®) Magnesium Gluconate Using LC-MS and NMR. *European Journal of Biophysics*. Vol. 5, No. 1, 2017, pp. 7-16.
doi: 10.11648/j.ejb.20170501.12

Received: January 31, 2017; **Accepted**: February 14, 2017; **Published**: February 25, 2017

Abstract: The current research work was designed to explore the impact of The Trivedi Effect® - Energy of Consciousness Healing Treatment (Biofield Energy Healing Treatment) on magnesium gluconate for the change in the structural properties and isotopic abundance ratio (P_{M+1}/P_M and P_{M+2}/P_M) by using LC-MS and NMR spectroscopy. Magnesium gluconate was divided into two parts – one part was control, and another part was treated with The Trivedi Effect®- Biofield Energy Healing Treatment remotely by seven renowned Biofield Energy Healers and defined as The Trivedi Effect® Treated sample. The LC-MS analysis of the both control and treated samples revealed the presence of the mass of the protonated magnesium gluconate at *m/z* 415 at the retention time of 1.53 min with similar fragmentation pattern. The relative peak intensities of the fragment ions of the treated sample were significantly changed compared with the control sample. The proton and carbon signals for CH, CH_2 and CO groups in the proton and carbon NMR spectra were found almost similar for the control and the treated samples. The isotopic abundance ratio analysis revealed that the isotopic abundance ratio of P_{M+1}/P_M ($^2H/^1H$ or $^{13}C/^{12}C$ or $^{17}O/^{16}O$ or $^{25}Mg/^{24}Mg$) in the treated sample was significantly increased by 34.33% compared with the control sample. Subsequently, the percentage change of the isotopic abundance ratio of P_{M+2}/P_M ($^{18}O/^{16}O$ or $^{26}Mg/^{24}Mg$) was significantly decreased in the treated sample by 64.08% as compared to the control sample. Briefly, ^{13}C, ^2H, ^{17}O, and ^{25}Mg contributions from $(C_{12}H_{23}MgO_{14})^+$ to *m/z* 416; ^{18}O and ^{26}Mg contributions from $(C_{12}H_{23}MgO_{14})^+$ to *m/z* 417 in the treated sample were significantly changed compared with the control sample. Thus, the treated magnesium gluconate could be valuable for designing better pharmaceutical and/or nutraceutical formulations through its changed physicochemical and thermal properties, which might be providing better therapeutic response against various diseases such as diabetes mellitus, allergy, aging, inflammatory diseases, immunological disorders, and other chronic infections. The Biofield Energy Treated magnesium gluconate might be supportive to design the novel potent enzyme inhibitors by using its kinetic isotope effects.

Keywords: Biofield Energy Healing Treatment, Consciousness Energy Healing Treatment, Biofield Energy Healers, The Trivedi Effect®, Magnesium Gluconate, LC-MS, NMR, Isotopic Abundance Ratio, Isotope Effects

1. Introduction

Magnesium ion (Mg^{2+}) is a major intracellular divalent cation. It is an essential mineral for several enzymes, DNA and RNA synthesis, reproduction and protein synthesis as well as a vital coherent controller of glycolysis and the Krebs cycle [1, 2]. Magnesium gluconate ($C_{12}H_{22}MgO_{14}$) is the organometallic salt of magnesium with gluconic acid produced from glucose catalyzed by glucose oxidase [3]. Magnesium gluconate is found to be the most powerful antioxidant than other magnesium salts and it is useful for the prevention and treatment of many diseases such as cardiovascular diseases, diabetes mellitus, allergy, inflammatory diseases, immunological disorders, Alzheimer's disease, asthma, pre-eclampsia and eclampsia, cancer, etc. [4-8]. It can be used as neuroprotective [9], for the treatment of oxidative stress induced ischemia/reperfusion injury [10] and also labor in women arrested initially with intravenous therapy as an oral tocolytic agent [11]. This organometallic salt can be used in a skin-tightening cosmetic composition [12]. Magnesium gluconate showed the highest bioavailability and most physiologically acceptable salt among other magnesium salts like chloride, sulfate, carbonate, acetate, citrate, lactate, aspartate, etc. [8, 13]. Therefore, magnesium gluconate was considered as one of the components in a novel proprietary herbomineral formulation for the source of magnesium ion. This herbomineral formulation which is designed as nutraceutical supplement can be used for the prevention and treatment of various human diseases.

Since ancient times, many different cultures, religions and systems of belief have recognized a living force that preserves and inhabits every living organism. This force is the source of 'life' and has been called various names, such as prana by the Hindus, *qi* or *chi* by the Chinese, and *ki* by the Japanese. This is believed to co-relate with the soul, spirit and mind. This hypothetical vital force has been scientifically evaluated and is now considered the Bioenergetics Field. The Biofield Energy is a dynamic electromagnetic field surrounding the human body, resulting from the continuous emission of low-level light, heat, and acoustical energy from the body. Biofield Energy is infinite, paradimensional and can freely flow between the human and environment [14, 15]. So, a human has the ability to harness energy from the ionosphere of the earth, the "universal energy field", and transmit it to any living organism(s) or nonliving object(s) around the globe. The object or recipient always receives the energy and responds in a useful way. This process is known as The Trivedi Effect® - Biofield Energy Healing Treatment [16, 17]. Biofield (Putative Energy Field) based Energy Therapies are used worldwide to promote health and healing. The National Center of Complementary and Integrative Health (NCCIH) has recognized and accepted Biofield Energy Healing as a Complementary and Alternative Medicine (CAM) health care approach in addition to other therapies, medicines and practices such as natural products, deep breathing, yoga, Tai Chi, Qi Gong, chiropractic/osteopathic manipulation, meditation, massage, special diets, homeopathy, progressive relaxation, guided imagery, acupressure, acupuncture, relaxation techniques, hypnotherapy, healing touch, movement therapy, pilates, rolfing structural integration, mindfulness, Ayurvedic medicine, traditional Chinese herbs and medicines, naturopathy, essential oils, aromatherapy, Reiki, cranial sacral therapy and applied prayer (as is common in all religions, like Christianity, Hinduism, Buddhism and Judaism) [18]. Biofield Energy Treatment (The Trivedi Effect®) has been extensively studied with significant outcomes in many scientific fields such as cancer research [19], altered antimicrobial sensitivity of pathogenic microbes in microbiology [20, 21], genetics [22, 23], biotechnology [24, 25], altered physical and chemical properties of pharmaceuticals [26, 27], nutraceuticals [28, 29], organic compounds [30, 31], improved overall growth and yield of plants in agricultural science [32, 33], and changing the structure of the atom in relation to various metals, ceramics, polymers and chemicals in materials science [34, 35]. The scientific study indicated that Biofield Energy Healing Treatment (The Trivedi Effect®) might be an alternate method for increasing or decreasing the natural isotopic abundance ratio of the substances [36-38]. The stable isotope ratio analysis has the wide applications in several scientific fields for understanding the isotope effects resulting from the variation of the isotopic composition of the molecule [39, 40]. Conventional mass spectrometry (MS) techniques such as liquid chromatography – mass spectrometry (LC-MS), gas chromatography – mass spectrometry (GC-MS) are widely used for isotope ratio analysis with sufficient precision [41]. Hence, LC-MS and NMR (Nuclear Magnetic Resonance) were used in this study to characterize the structural properties of the Biofield Energy Treated and untreated magnesium gluconate qualitatively for the purpose of the pharmaceutical and nutraceutical industrial applications. Consequently, LC-MS based isotopic abundance ratio (P_{M+1}/P_M and P_{M+2}/P_M) analysis in both the Biofield Energy Treated and untreated samples was designed to investigate the influence of The Trivedi Effect® - Energy of Consciousness Healing Treatment on the isotopic abundance ratio in magnesium gluconate.

2. Materials and Methods

2.1. Chemicals and Reagents

Magnesium gluconate hydrate was purchased from Tokyo Chemical Industry Co., Ltd. (TCI), Japan. All other chemicals used in the experiment were of analytical grade available in India.

2.2. Energy of Consciousness Healing Treatment Strategies

Magnesium gluconate hydrate was one of the components of the new proprietary herbomineral formulation, which was

developed by our research team and was used *per se* as the test compound for the current study. The test compound was divided into two parts, one part of the test compound did not receive any sort of treatment and was defined as the untreated or control magnesium gluconate sample. The second part of the test compound, which was denoted as the Biofield Energy Treated sample, was treated with the Biofield Energy by the group of seven renowned Biofield Energy Healers (The Trivedi Effect®) remotely. Six Biofield Energy Healers were remotely located in the U.S.A. and one of which was remotely located in Canada, while the test compound was located in the research laboratory of GVK Biosciences Pvt. Ltd., Hyderabad, India. This Biofield Treatment was provided for 5 minutes through the Healer's Unique Energy Transmission process remotely to the test compound, which was kept under laboratory conditions. None of the Biofield Energy Healers in this study visited the laboratory in person, nor had any contact with the compounds. Similarly, the control compound was subjected to "sham" healer for 5 minutes, under the same laboratory conditions. The sham healer did not have any knowledge about the Biofield Energy Treatment. After that, the Biofield Energy Treated and untreated samples were kept in similar sealed conditions and characterized thoroughly by LC-MS and NMR spectroscopy.

2.3. Characterization

2.3.1. Liquid Chromatography Mass Spectrometry (LC-MS) Analysis

Liquid chromatography was performed using The Waters® ACQUITY UPLC, Milford, MA, USA equipped with a binary pump (The Waters® BSM HPLC pump), autosampler, column heater and a photo-diode array (PDA) detector. The column used for the study was a reversed phase Acquity BEH shield RP C18 (150 X 3.0 mm, 2.5 µm). The column temperature was kept constant at 40˚C. The mobile phase was 2mM ammonium acetate in water as mobile phase A and acetonitrile as mobile phase B. Chromatographic separation was achieved with following gradient program: 0 min – 5%B; 1 min – 5%B; 15 min - 97%B; 20 min – 97%B; 21 min – 5%B; 25 min – 5%B. The flow rate was at a constant flow rate of 0.4 mL/min. The control and Biofield Energy Treated samples were dissolved in a mixture of water and methanol (60:40 *v/v*) to prepare a 1 mg/mL stock solution. An aliquot of 2 µL of the stock solution was used for analysis by LC-ESI-MS and the total run time was 25 min.

Mass spectrometric analysis was accompanied on a Triple Quad (Waters Quattro Premier XE, USA) mass spectrometer equipped with an electrospray ionization (ESI) source with the following parameters: electrospray capillary voltage 3.5 kV; source temperature 100°C; desolvation temperature 350°C; cone voltage 30 V; desolvation gas flow 1000 L/h and cone gas flow 60 L/h. Nitrogen was used in the electrospray ionization source. The multiplier voltage was set at 650 V. LC-MS was taken in positive ionization mode and with the full scan (*m/z* 50-1400). The total ion chromatogram, % peak area and mass spectrum of the individual peak (appeared in LC) were recorded.

2.3.2. Isotopic Abundance Ratio Analysis

The relative intensity of the peak in the mass spectra is directly proportional to the relative isotopic abundance of the molecule and the isotopic abundance ratio analysis was followed the scientific literature reported [36-38, 42] method described as below:

P_M stands for the relative peak intensity of the parent molecular ion $[M^+]$ expressed in percentage. In other way, it indicates the probability to *A elements* having only one natural isotope in appreciable abundance (for *e.g.* ^{12}C, ^{1}H, ^{16}O, ^{24}Mg, etc.) contributions to the mass of the parent molecular ion $[M^+]$.

P_{M+1} represents the relative peak intensity of the isotopic molecular ion $[(M+1)^+]$ expressed in percentage

$$= (\text{no. of } ^{13}C \times 1.1\%) + (\text{no. of } ^{15}N \times 0.40\%) + (\text{no. of } ^{2}H \times 0.015\%) + (\text{no. of } ^{17}O \times 0.04\%) + (\text{no. of } ^{25}Mg \times 12.66\%)$$

i.e. the probability to *A + 1 elements* having an isotope that has one mass unit heavier than the most abundant isotope (for *e.g.* ^{13}C, ^{2}H, ^{17}O, ^{25}Mg, etc.) contributions to the mass of the isotopic molecular ion $[(M+1)^+]$.

P_{M+2} represents the relative peak intensity of the isotopic molecular ion $[(M+2)^+]$ expressed in the percentage

$$= (\text{no. of } ^{18}O \times 0.20\%) + (\text{no. of } ^{26}Mg \times 13.94\%)$$

i.e. the probability to have *A* + 2 *elements* having an isotope that has two mass unit heavier than the most abundant isotope (for *e.g.* ^{18}O, ^{26}Mg, etc.) contributions to the mass of isotopic molecular ion $[(M+2)^+]$.

Table 1. *The isotopic composition (i.e. the natural isotopic abundance) of the elements.*

Element	Symbol	Mass	% Natural Abundance	*A*+1 Factor	*A*+2 Factor
Hydrogen	^{1}H	1	99.9885		
	^{2}H	2	0.0115	$0.015n_H$	
Carbon	^{12}C	12	98.892		
	^{13}C	13	1.108	$1.1\ n_C$	
Oxygen	^{16}O	16	99.762		
	^{17}O	17	0.038	$0.04\ n_O$	
	^{18}O	18	0.200		$0.20\ n_O$
Magnesium	^{24}Mg	24	78.99		
	^{25}Mg	25	10.00	$12.66\ n_{Mg}$	
	^{26}Mg	26	11.01		$13.94\ n_{Mg}$

A represents element, n represents the number of the element (*i.e.* C, H. O, Mg, etc.)

The value of the natural isotopic abundance of the elements used here for the theoretical calculation are achieved from the scientific literature and presented in the Table 1 [43, 44].

Isotopic abundance ratio for *A* + 1 *elements* = P_{M+1}/P_M

Similarly, isotopic abundance ratio for *A* + 2 *elements* = P_{M+2}/P_M

Percentage (%) change in isotopic abundance ratio = $[(IAR_{Treated} - IAR_{Control})/ IAR_{Control}) \times 100]$,

Where, $IAR_{Treated}$ = isotopic abundance ratio in the Biofield Energy Treated sample and $IAR_{Control}$ = isotopic abundance ratio in the control sample.

2.3.3. Nuclear Magnetic Resonance (NMR) Analysis

^{1}H NMR spectra were recorded in a 400 MHZ VARIAN FT-NMR spectrometer at room temperature. Data refer to solutions in D_2O with the residual solvent protons as internal references. ^{1}H NMR multiplicities were designated as singlet (s), doublet (d), triplet (t), multiplet (m), and broad (br). ^{13}C NMR spectra were measured at 100 MHz on a VARIAN FT-NMR spectrometer at room temperature. Chemical shifts (δ) were in parts per million (ppm) relative to the solvent's residual proton chemical shift (D_2O, δ = 4.65 ppm) and solvent's residual carbon chemical shift (D_2O, δ = 0 ppm).

3. Results and Discussion

3.1. Liquid Chromatography-Mass Spectrometry (LC-MS) Analysis

The liquid chromatograms of both the control and Biofield Energy Treated magnesium gluconate

(Figure 1) exhibited a sharp peak at the retention time (R_t) of 1.53 min. This result clearly indicated that the polarity/affinity of the Biofield Energy Treated sample remained unchanged compared with the control sample. The ESI-MS spectra of both the control and Biofield Energy Treated magnesium gluconate at R_t of 1.53 min as shown in the Figure 2 revealed the presence of the mass of the magnesium gluconate at *m/z* 415 $[M + H]^+$ (calcd for $C_{12}H_{23}MgO_{14}^+$, 415).

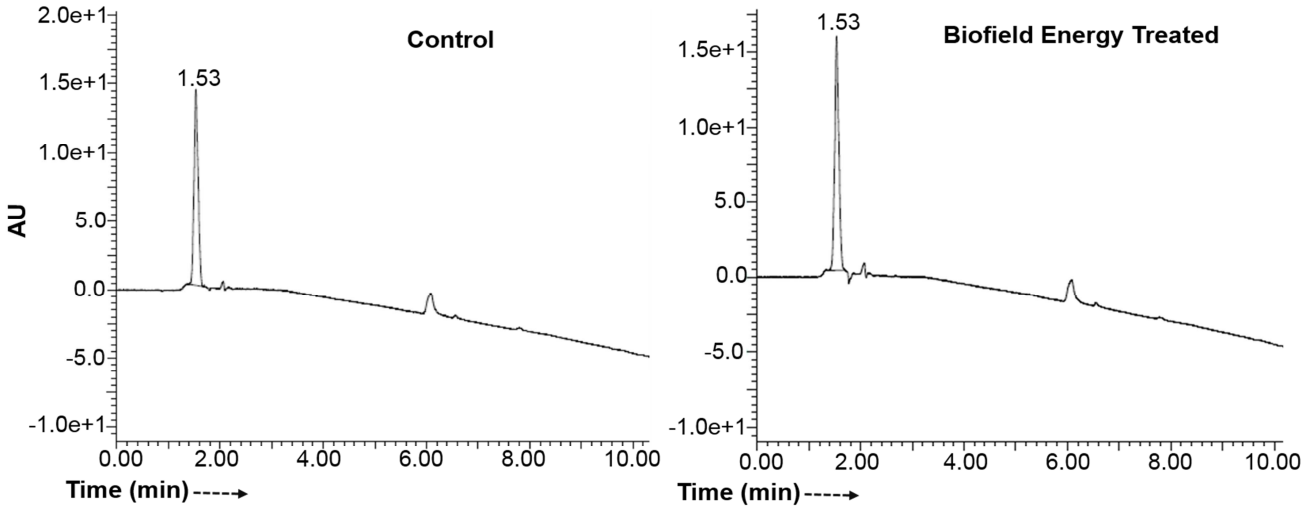

Figure 1. *Liquid chromatograms of the control and Biofield Energy Treated magnesium gluconate.*

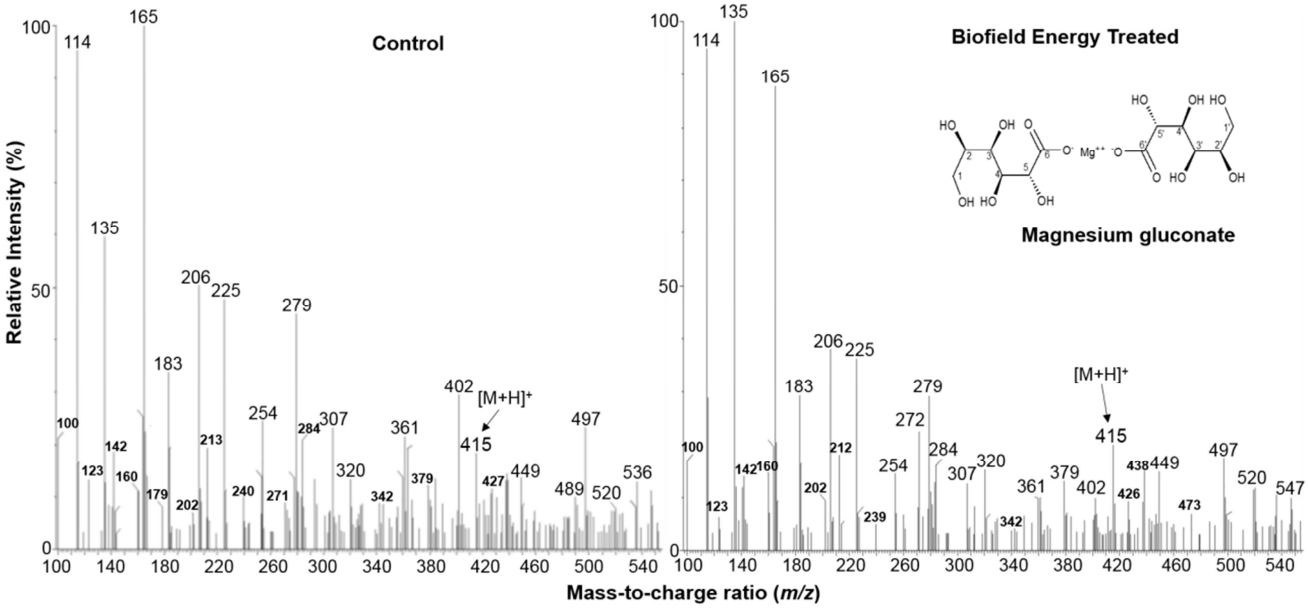

Figure 2. *The ESI-MS spectra of the control and Biofield Energy Treated magnesium gluconate.*

The distinctive fragmented ion peaks in the lower *m/z* region of the protonated magnesium gluconate ion at *m/z* 415 were observed in both the control and Biofield Energy Treated samples at *m/z* 402 $[M - H_2O + 6H]^+$ (calcd for

$C_{12}H_{26}MgO_{13}^{4+}$, 402), 379 [M – $2H_2O$ + H]$^+$ (calcd for $C_{12}H_{19}MgO_{12}^{+}$, 379), 361 [M – $3H_2O$ + H]$^+$ (calcd for $C_{12}H_{17}MgO_{11}^{+}$, 361), 342 [M – $4H_2O$]$^+$ (calcd for $C_{12}H_{14}MgO_{10}^{2+}$, 342) as shown in the Figure 3.

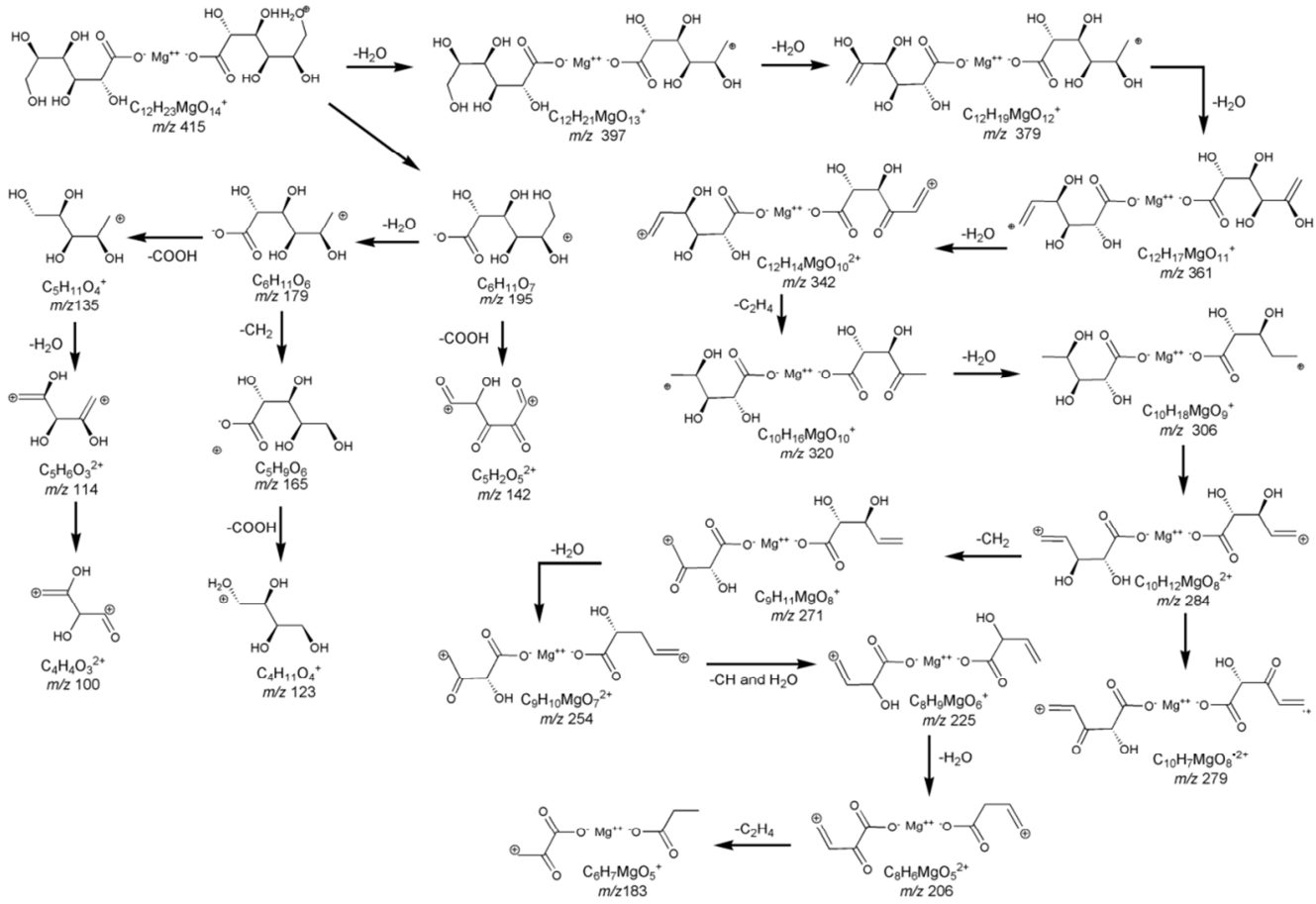

Figure 3. *Proposed fragmentation pathway of magnesium gluconate.*

By this way removing water along with other groups like alkyl, magnesium gluconate produces different fragmentation ion peaks at *m/z* 320, 307, 284, 279, 271, 254, 225, 206, 183, 179, 165, 142, 135, 123, 114, and 100 which were observed in the ESI-MS spectra of both the control and Biofield Energy Treated samples (Figure 2). These ions correspond to the following proposed molecular formula $C_{10}H_{16}MgO_{10}^{+}$, $C_{10}H_{19}MgO_9^{+}$, $C_{10}H_{12}MgO_8^{2+}$, $C_{10}H_7MgO_8^{\bullet 2+}$, $C_9H_{11}MgO_8^{+}$, $C_9H_{10}MgO_7^{2+}$, $C_8H_9MgO_6^{+}$, $C_8H_6MgO_5^{2+}$, $C_6H_7MgO_5^{+}$, $C_6H_{11}O_6^{+}$, $C_5H_9O_6^{+}$, $C_5H_2O_5^{2+}$, $C_5H_{11}O_4^{+}$, $C_4H_{11}O_4^{+}$, $C_5H_6O_3^{2+}$, and $C_4H_4O_3^{2+}$, respectively as shown in Figure 3. The ESI-MS spectra of both the control and Biofield Energy Treated samples (Figure 2) exhibited that the fragmentation pattern of both the control and Biofield Energy Treated samples were the same. The fragmented ion at *m/z* 165 corresponding to $C_5H_9O_6^{+}$ exhibited 100% relative peak intensity in the control sample, while fragment ion at *m/z* 135 corresponding to $C_5H_{11}O_4^{+}$ showed 100% relative peak intensity in the Biofield Energy Treated sample (Figure 2). The relative peak intensities of the Biofield Energy Treated sample were significantly altered compared with the control sample.

3.2. Isotopic Abundance Ratio Analysis

The molecular formula of magnesium gluconate is $C_{12}H_{22}MgO_{14}$. But, in the ESI-MS spectra, it existed as a protonated molecular ion at *m/z* 415 ($C_{12}H_{23}MgO_{14}^{+}$) showing 18.46% (control) and 19.91% (Biofield Energy Treated) relative intensity. The theoretical calculation of P_{M+1} and P_{M+2} for the protonated magnesium gluconate was presented as below:

$$P\ (^{13}C) = [(12 \times 1.1\%) \times 18.46\% \text{ (the actual size of the } M^+ \text{ peak)}] / 100\% = 2.44\%$$

$$P\ (^{2}H) = [(23 \times 0.015\%) \times 18.46\%] / 100\% = 0.06\%$$

$$P\ (^{17}O) = [(14 \times 0.04\%) \times 18.46\%] / 100\% = 0.10\%$$

$$P\ (^{25}Mg) = [(1 \times 12.66\%) \times 18.46\%] / 100\% = 2.34\%$$

P_{M+1} *i.e.* ^{13}C, ^{2}H, ^{17}O, and ^{25}Mg contributions from $(C_{12}H_{23}MgO_{14})^{+}$ to *m/z* 416 = 4.94%

From the above calculation, it has been found that ^{13}C and ^{25}Mg have major contribution to *m/z* 416.

In the similar approach, P_{M+2} can be calculated as follow:

$$P\ (^{18}O) = [(14 \times 0.20\%) \times 18.46\%] / 100\% = 0.52\%$$

P (^{26}Mg) = [(1 x 13.94%) x 18.46%] / 100% = 2.57%

So, P_{M+2} *i.e.* ^{18}O and ^{26}Mg contributions from $(C_{12}H_{23}MgO_{14})^+$ to *m/z* 417 = 3.09%.

But the experimental data showed the difference due to the complexity in the structure. LC-MS spectra of the control and Biofield Energy Treated samples indicated the presence of the mass for the protonated magnesium gluconate itself (*m/z* 415). Hence, P_M, P_{M+1}, P_{M+2} for magnesium gluconate at *m/z* 415, 416 and 417 of the control and Biofield Energy Treated samples were obtained from the observed relative peak intensities of $[M^+]$, $[(M+1)^+]$, and $[(M+2)^+]$ peaks, respectively in the respective ESI-MS spectra and are presented in Table 2.

Table 2. *Isotopic abundance analysis results of the magnesium gluconate ion in the control and Biofield Energy Treated sample.*

Parameter	Control sample	Biofield Energy Treated sample
P_M at *m/z* 415 (%)	18.46	19.91
P_{M+1} at *m/z* 416 (%)	6.06	8.78
P_{M+1}/P_M	0.3283	0.4410
% Change of isotopic abundance ratio (P_{M+1}/P_M) with respect to the control sample		34.33
P_{M+2} at *m/z* 417 (%)	8.65	3.35
P_{M+2}/P_M	0.4686	0.1683
% Change of isotopic abundance ratio (P_{M+2}/P_M) with respect to the control sample		-64.08

P_M = the relative peak intensity of the parent molecular ion $[M^+]$; P_{M+1} = the relative peak intensity of the isotopic molecular ion $[(M+1)^+]$, P_{M+2} = the relative peak intensity of the isotopic molecular ion $[(M+2)^+]$, and M = mass of the parent molecule.

The isotopic abundance ratio of P_{M+1}/P_M in the Biofield Energy Treated sample was significantly increased by 34.33% with respect to the control sample (Table 2). Consequently, the percentage change of the isotopic abundance ratio of P_{M+2}/P_M was remarkably decreased by 64.08% in the Biofield Energy Treated sample compared with the control sample (Table 2). So, ^{13}C, ^{2}H, ^{17}O, and ^{25}Mg contributions from $(C_{12}H_{23}MgO_{14})^+$ to *m/z* 416; ^{18}O and ^{26}Mg contributions from $(C_{12}H_{23}MgO_{14})^+$ to *m/z* 417 in the Biofield Energy Treated sample were significantly changed compared with the control sample.

Table 3. *Possible isotopic bond and their effect in the vibrational energy in magnesium gluconate molecule.*

SL No.	Probable isotopic bond	Isotope type	Reduced mass (μ)	Zero point vibrational energy (E_0)
1	^{12}C-^{12}C	Lighter	6.00	Higher
2	^{13}C-^{12}C	Heavier	6.26	Smaller
3	^{1}H-^{12}C	Lighter	0.92	Higher
4	^{2}H-^{12}C	Heavier	1.04	Smaller
5	^{12}C-^{16}O	Lighter	6.86	Higher
6	^{13}C-^{16}O	Heavier	7.17	Smaller
7	^{12}C-^{17}O	Heavier	7.03	Smaller
8	^{12}C-^{18}O	Heavier	7.20	Smaller
9	^{16}O-^{1}H	Lighter	0.94	Higher
10	^{16}O-^{2}H	Heavier	1.78	Smaller
11	^{24}Mg-^{16}O	Lighter	9.60	Higher
12	^{25}Mg-^{16}O	Heavier	9.76	Smaller
13	^{26}Mg-^{16}O	Heavier	9.91	Smaller
14	^{24}Mg-^{17}O	Heavier	9.95	Smaller
15	^{24}Mg-^{18}O	Heavier	10.29	Smaller

Scientific literature [40-42, 45] reported that the vibrational energy is closely related with the reduced mass (μ) of the compound and the alteration of the vibrational energy can affect the several properties like physicochemical, thermal properties of the molecule. The relation between the vibrational energy and the reduced mass (μ) for a diatomic molecule is expressed as below (Equation 1) [40, 45]:

$$E_o = \frac{h}{4\pi}\sqrt{\frac{f}{\mu}} \quad (1)$$

Where E_0 = the vibrational energy of a harmonic oscillator at absolute zero or zero point energy

f = force constant

$$\mu = \text{reduced mass} = \frac{m_a m_a}{m_a + m_a}$$

Where m_a and m_b are the masses of the constituent atoms.

The alteration in the isotopic abundance ratios of ^{13}C/^{12}C for C-O; ^{2}H/^{1}H for C-H and O-H bonds; ^{17}O/^{16}O and ^{18}O/^{16}O for C-O bond; ^{25}Mg/^{24}Mg, ^{26}Mg/^{24}Mg, ^{17}O/^{16}O and ^{18}O/^{16}O for Mg-O bond have the significant impact on the ground state vibrational energy of the molecule due to the higher reduced mass (μ) as shown in the Table 4 that leads to the isotope effects of the molecule.

Mass spectroscopic analysis of the several organic compounds revealed that the isotopic abundance of $[M+1]^+$ and $[M+2]^+$ ions were increased or decreased, thereby suggesting the change in number of neutrons in the molecule. It was then postulated to the alterations in atomic mass and atomic charge through possible mediation of neutrino oscillation [46, 47]. It is then assumed that The Trivedi Effect® - Energy of Consciousness Healing Treatment might provide the required energy for the neutrino oscillations. The changes of neutrinos inside the molecule in turn modified the particle size, chemical reactivity, density, thermal behavior, selectivity, binding energy etc. [46]. Kinetic isotope effect that is resultant from the variation in the isotopic abundance ratio of one of the atoms in the reactants in a chemical reaction is very useful to study the reaction mechanism as well as for understanding the enzymatic transition state and

all aspects of enzyme mechanism that is supportive for designing enormously effective and specific inhibitors [40, 45, 48]. As magnesium is an essential cofactor for various enzymatic reactions, Biofield Energy Treated magnesium gluconate that had altered isotopic abundance ratio might be advantageous for the study of enzyme mechanism as well as support in the designing of novel potent enzyme inhibitors.

3.3. Nuclear Magnetic Resonance (NMR) Analysis

The ^{1}H and ^{13}C NMR spectra of the control and Biofield Energy Treated magnesium gluconate are presented in the Figures 4 and 5, respectively. NMR assignments of the control and Biofield Energy Treated magnesium gluconate are presented in the Table 4.

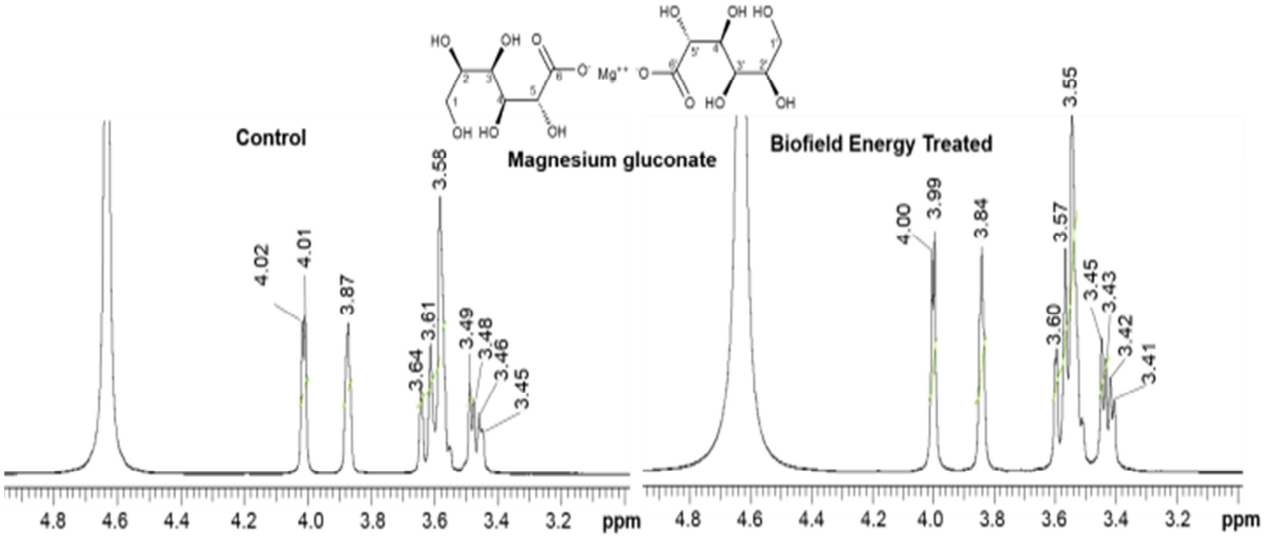

Figure 4. *The ^{1}H NMR spectra of the control and Biofield Energy Treated magnesium gluconate.*

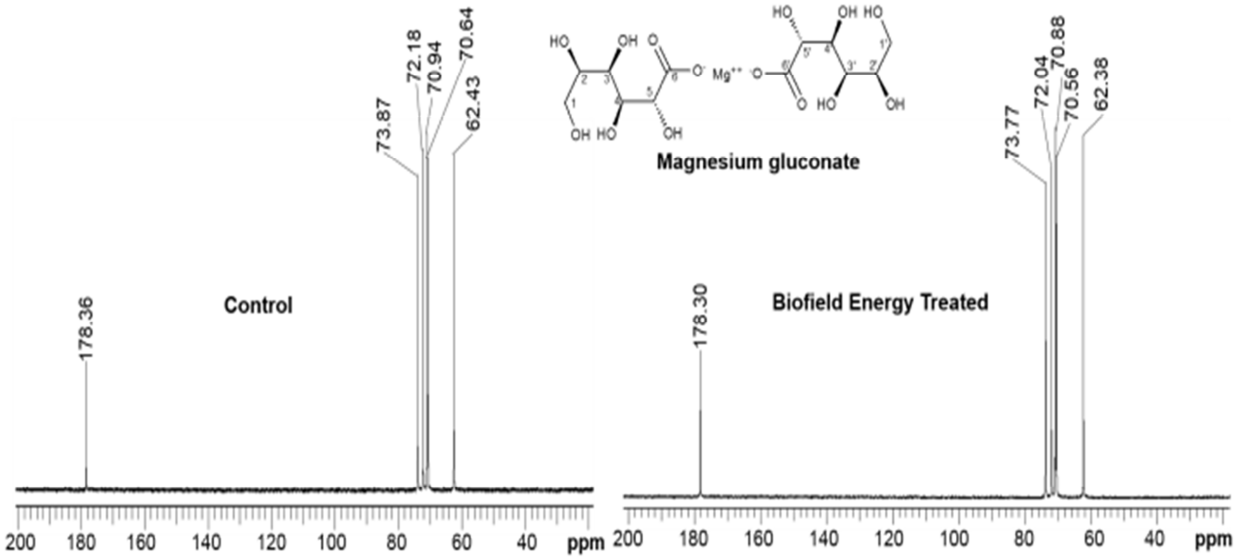

Figure 5. *The ^{13}C NMR spectra of the control and Biofield Energy Treated magnesium gluconate.*

Table 4. *^{1}H NMR and ^{13}C NMR spectroscopic data of both the control and Biofield Energy Treated of magnesium gluconate.*

Position	^{1}H NMR δ (ppm)			^{13}C NMR δ (ppm)	
	Number	Control	Treated	Control	Treated
1, 1'	4H*	3.64 (br s), 3.47 (dd, *J* = 12, 4 Hz)	3.60 (br s), 3.43 (dd, *J* =12, 4 Hz)	62.43	62.38
2, 2'	2H*	3.58 (br s)	3.55 (br s)	70.64	70.56
3, 3'	2H*	3.61 (br s)	3.57 (br s)	70.94	70.88
4, 4'	2H	3.87 (br s)	3.84 (br s)	72.18	72.04
5, 5'	2H	4.015 (d, *J* = 4 Hz)	3.995 (d, *J* = 4 Hz)	73.87	73.77
6, 6'	--		--	178.36	178.30

br- broad, s- singlet, and m- multiplet, * These assignments can be switched.

Although magnesium gluconate contains a large number of hydroxyl (OH) groups, the proton spectra of both the control and Biofield Energy Treated samples did not show any signal for the hydroxyl protons. The scientific literature mentioned that when deuterated water was used as solvent for spectra recording, the hydroxyl protons were replaced by deuterium from deuterated water. The signals for the protons coupling of CH_2 group and adjacent CH protons (2-5) in the gluconic acid portion were observed in the range of δ 3.60-4.20 ppm in the proton spectrum of sodium gluconate [49]. The proton signals for CH_2 and CH groups for the control sample were observed in the range of δ 3.47-4.015 ppm (Table 4), whereas these signals were noticed in the Biofield Energy Treated in the range of δ 3.43-3.995 ppm. Similarly, the carbon signals for CO group, CH_2 and CH groups in the ^{13}C NMR spectrum of the Biofield Energy Treated sample were slightly decreased compared with the control sample (Table 4). These results indicated that the structure of the magnesium gluconate remained unchanged due to the Biofield Energy Healing Treatment.

4. Conclusions

The current study successfully demonstrated the structural characterization of magnesium gluconate by using LC-MS and NMR techniques and a significantly impact of The Trivedi Effect®- Energy of Consciousness Healing Treatment (Biofield Energy Healing Treatment) on the isotopic abundance ratios of P_{M+1}/P_M and P_{M+2}/P_M. The LC-MS analysis of the both control and Biofield Energy Treated samples revealed the presence of the mass of the protonated magnesium gluconate at *m/z* 415 at the retention time of 1.53 min with similar fragmentation pattern. The relative peak intensities of the fragment ions of the treated sample were significantly changed compared with the control sample. The isotopic abundance ratio of P_{M+1}/P_M ($^2H/^1H$ or $^{13}C/^{12}C$ or $^{17}O/^{16}O$ or $^{25}Mg/^{24}Mg$) in the treated sample was significantly increased by 34.33% compared with the control sample. Subsequently, the percentage change of the isotopic abundance ratio of P_{M+2}/P_M ($^{18}O/^{16}O$ or $^{26}Mg/^{24}Mg$) was significantly decreased in the treated sample by 64.08% as compared to the control sample. Briefly, ^{13}C, ^2H, ^{17}O, and ^{25}Mg contributions from $(C_{12}H_{23}MgO_{14})^+$ to *m/z* 416; ^{18}O and ^{26}Mg contributions from $(C_{12}H_{23}MgO_{14})^+$ to *m/z* 417 in the treated sample were significantly altered with respect to the control sample. The treated sample might exhibit isotope effects such as altered physicochemical and thermal properties, rate of the reaction, selectivity and binding energy due to its changed isotopic abundance ratios of P_{M+1}/P_M and P_{M+2}/P_M as compared to the control sample. The treated magnesium gluconate might be helpful to understand the enzymatic reactions as well as design the novel potent enzyme inhibitors by using its kinetic isotope effects. Besides, The Trivedi Effect® - Energy of Consciousness Healing Treatment, could be a useful approach in the design of better nutraceutical and/or pharmaceutical formulations that can offer significant therapeutic responses against various diseases such as diabetes mellitus, allergies and septic shock; stress-related disorders like sleep disorder, insomnia, anxiety, depression, Attention Deficit Disorder (ADD), Attention Deficit Hyperactive Disorder (ADHD), mental restlessness (mind chattering), brain frog, low libido, impotency, lack of motivation, mood swings, fear of the future, confusion, migraines, headaches, forgetfulness, overwhelm, loneliness, worthlessness, indecisiveness, frustration, irritability, chronic fatigue, obsessive/compulsive behavior and panic attacks; inflammatory diseases and immunological disorders like Lupus, Systemic Lupus Erythematosus, Hashimoto Thyroiditis, Type 1 Diabetes, Asthma, Chronic peptic ulcers, Tuberculosis, Hepatitis, Chronic active hepatitis, Celiac Disease (gluten-sensitive enteropathy), Addison Disease, Crohn's disease, Graves' Disease, Pernicious and Aplastic Anemia, Sjogren Syndrome, Irritable Bowel Syndrome (IBS), Multiple Sclerosis, Rheumatoid arthritis, Chronic periodontitis, Ulcerative colitis, Chronic sinusitis, Myasthenia Gravis, Atherosclerosis, Vasculitis, Dermatitis, Diverticulitis, Rheumatoid Arthritis, Reactive Arthritis, Alopecia Areata, Psoriasis, Scleroderma, Fibromyalgia, Chronic Fatigue Syndrome and Vitiligo; aging-related diseases like cardiovascular disease, arthritis, cancer, Alzheimer's disease, dementia, cataracts, osteoporosis, diabetes, hypertension, glaucoma, hearing loss, Parkinson's Disease, Huntington's Disease, Prion Disease, Motor Neurone Disease, Spinocerebellar Ataxia, Spinal muscular atrophy, Amyotrophic lateral sclerosis, Friedreich's Ataxia and Lewy Body Disease; chronic infections and much more.

Abbreviations

A: Element; LC-MS: Liquid chromatography-mass spectrometry; M: Mass of the parent molecule; *m/z*: Mass-to-charge ratio; n: Number of the element; NMR: Nuclear magnetic resonance spectroscopy; P_M: The relative peak intensity of the parent molecular ion $[M^+]$; P_{M+1}: The relative peak intensity of isotopic molecular ion $[(M+1)^+]$); P_{M+2}: The relative peak intensity of isotopic molecular ion $[(M+2)^+]$); R_t: Retention time.

Acknowledgements

The authors are grateful to GVK Biosciences Pvt. Ltd., Trivedi Science, Trivedi Global, Inc. and Trivedi Master Wellness for their assistance and support during this work.

References

[1] Heaton FW (1990) Role of magnesium in enzyme systems in metal ions in biological systems, In: Sigel H, Sigel A (Eds.), Volume 26: Compendium on magnesium and its role in biology, nutrition and physiology, Marcel Dekker Inc., New York.

[2] Garfinkel L, Garfinkel D (1985) Magnesium regulation of the glycolytic pathway and the enzymes involved. Magnesium 4: 60-72.

[3] Ramachandran S, Fontanille P, Pandey A, Larroche C (2006) Gluconic acid: Properties, applications and microbial production. Food Technol Biotechnol 44: 185-195.

[4] Gröber U, Schmidt J, Kisters K (2015) Magnesium in prevention and therapy. Nutrients 7: 8199-8226.

[5] William JH, Danziger J (2016) Magnesium deficiency and proton-pump inhibitor use: A clinical review. J Clin Pharmacol 56: 660-668.

[6] Guerrera MP, Volpe SL, Mao JJ (2009) Therapeutic uses of magnesium. Am Fam Physician 80: 157-162.

[7] Fleming TE, Mansmann Jr HC (1999) Methods and compositions for the prevention and treatment of diabetes mellitus. United States Patent 5871769, 1-10.

[8] Fleming TE, Mansmann Jr HC (1999) Methods and compositions for the prevention and treatment of immunological disorders, inflammatory diseases and infections. United States Patent 5939394, 1-11.

[9] Turner RJ, Dasilva KW, O'Connor C, van den Heuvel C, Vink R (2004) Magnesium gluconate offers no more protection than magnesium sulphate following diffuse trau-matic braininjury in rats. J Am Coll Nutr 23: 541S-544S.

[10] Weglicki WB (2000) Intravenous magnesium gluconate for treatment of conditions caused by excessive oxidative stress due to free radical distribution. United States Patent 6100297, 1-6.

[11] Martin RW, Martin JN Jr, Pryor JA, Gaddy DK, Wiser WL, Morrison JC (1988) Comparison of oral ritodrine and magnesium gluconate for ambulatory tocolysis. Am J Obstet Gynecol 158: 1440-1445.

[12] Lee KH, Chung SH, Song JH, Yoon JS, Lee J, Jung MJ, Kim JH (2013) Cosmetic compositions for skin-tightening and method of skin-tightening using the same. United States Patent 8580741 B2.

[13] Coudray C, Rambeau M, Feillet-Coudray C, Gueux E, Tressol JC, Mazur A, Rayssiguier Y (2005) Study of magnesium bioavailability from ten organic and inorganic Mg salts in Mg-depleted rats using a stable isotope approach. Magnes Res 18: 215-223.

[14] Stenger VJ (1999) Bioenergetic Fields. The Scientific Review of Alternative Medicine 3.

[15] Rogers, M (1989) "Nursing: A Science of Unitary Human Beings." In J.P. Riehl-Sisca (ed.) Conceptual Models for Nursing Practice. 3rd Edn. Norwark: Appleton & Lange.

[16] Rosa L, Rosa E, Sarner L, Barrett S (1998) A close look at therapeutic touch. JAMA- J Am Med Assoc 279: 1005-1010.

[17] Warber SL, Cornelio D, Straughn, J, Kile G (2004) Biofield energy healing from the inside. J Altern Complement Med 10: 1107-1113.

[18] Koithan M (2009) Introducing complementary and alternative therapies. J Nurse Pract 5: 18-20.

[19] Trivedi MK, Patil S, Shettigar H, Mondal SC, Jana S (2015) The potential impact of biofield treatment on human brain tumor cells: A time-lapse video microscopy. J Integr Oncol 4: 141.

[20] Trivedi MK, Branton A, Trivedi D, Nayak G, Mondal SC, Jana S (2015) Antibiogram of biofield-treated *Shigella boydii*: Global burden of infections. Science Journal of Clinical Medicine 4: 121-126.

[21] Trivedi MK, Branton A, Trivedi D, Nayak G, Shettigar H, Mondal SC, Jana S (2015) Antibiogram pattern of *Shigella flexneri*: Effect of biofield treatment. Air Water Borne Diseases 3: 122.

[22] Trivedi MK, Branton A, Trivedi D, Nayak G, Gangwar M, Jana S (2015) Characterization of phenotype and genotype of biofield treated *Enterobacter aerogenes*. Transl Med 5: 155.

[23] Trivedi MK, Branton A, Trivedi D, Nayak G, Gangwar M, Jana S (2015) Antibiogram and genotypic analysis using 16S rDNA after biofield treatment on *Morganella morganii*. Adv Tech Biol Med 3: 137.

[24] Trivedi MK, Branton A, Trivedi D, Nayak G, Bairwa K, Jana S (2015) Physicochemical and spectroscopic properties of biofield energy treated protose. American Journal of Biomedical and Life Sciences 3: 104-110.

[25] Trivedi MK, Branton A, Trivedi D, Nayak G, Gangwar M, Jana S (2015) Bacterial identification using 16S rDNA gene sequencing and antibiogram analysis on biofield treated *Pseudomonas fluorescens*. Clin Med Biochemistry Open Access 1: 101.

[26] Trivedi MK, Branton A, Trivedi D, Nayak G, Singh R, Jana S (2015) Characterisation of physical, spectral and thermal properties of biofield treated resorcinol. Organic Chem Curr Res 4:146.

[27] Trivedi MK, Branton A, Trivedi D, Nayak G, Bairwa K, Jana S (2015) Spectroscopic characterization of disulfiram and nicotinic acid after biofield treatment. J Anal Bioanal Tech 6: 265.

[28] Trivedi MK, Tallapragada RM, Branton A, Trivedi D, Nayak G, Latiyal O, Jana S (2015) Potential impact of biofield treatment on atomic and physical characteristics of magnesium. Vitam Miner 3: 129.

[29] Trivedi MK, Tallapragada RM, Branton A, Trivedi D, Nayak G, Latiyal O, Jana S (2015) Physical, Atomic and Thermal Properties of Biofield Treated Lithium Powder. J Adv Chem Eng 5: 136.

[30] Trivedi MK, Branton A, Trivedi D, Nayak G, Singh R, Jana S (2015) Experimental Investigation on Physical, Thermal and Spectroscopic Properties of 2-Chlorobenzonitrile: Impact of Biofield Treatment. Modern Chemistry 3: 38-46.

[31] Trivedi MK, Branton A, Trivedi D, Nayak G, Singh R, Jana S (2015) Characterization of physical, thermal and spectroscopic properties of biofield energy treated *p*-phenylenediamine and *p*-toluidine. J Environ Anal Toxicol 5: 329.

[32] Trivedi MK, Branton A, Trivedi D, Nayak G, Gangwar M, Jana S (2015) Agronomic characteristics, growth analysis, and yield response of biofield treated mustard, cowpea, horse gram, and groundnuts. International Journal of Genetics and Genomics 3: 74-80.

[33] Trivedi MK, Branton A, Trivedi D, Nayak G, Mondal SC, Jana S (2015) Evaluation of biochemical marker - glutathione and DNA fingerprinting of biofield energy treated *Oryza sativa*. American Journal of BioScience 3: 243-248.

[34] Trivedi MK, Nayak G, Tallapragada RM, Patil S, Latiyal O, Jana S (2015) Effect of biofield treatment on structural and morphological properties of silicon carbide. J Powder Metall Min 4: 132.

[35] Trivedi MK, Tallapragada RM, Branton A, Trivedi D, Nayak G, Latiyal O, Jana S (2015) Evaluation of atomic, physical and thermal properties of tellurium powder: Impact of biofield energy treatment. J Electr Electron Syst 4: 162.

[36] Trivedi MK, Branton A, Trivedi D, Nayak G, Sethi KK, Jana S (2016) Isotopic abundance ratio analysis of biofield energy treated indole using gas chromatography-mass spectrometry. Science Journal of Chemistry 4: 41-48.

[37] Trivedi MK, Branton A, Trivedi D, Nayak G, Panda P, Jana S (2016) Evaluation of the isotopic abundance ratio in biofield energy treated resorcinol using gas chromatography-mass spectrometry technique. Pharm Anal Acta 7: 481.

[38] Trivedi MK, Branton A, Trivedi D, Nayak G, Saikia G, Jana S (2016) Determination of isotopic abundance of ^{2}H, ^{13}C, ^{18}O, and ^{37}Cl in biofield energy treated dichlorophenol isomers. Science Journal of Analytical Chemistry 4: 1-6.

[39] Schellekens RC, Stellaard F, Woerdenbag HJ, Frijlink HW, Kosterink JG (2011) Applications of stable isotopes in clinical pharmacology. Br J Clin Pharmacol 72: 879-897.

[40] Muccio Z, Jackson GP (2009) Isotope ratio mass spectrometry. Analyst 134: 213-222.

[41] Vanhaecke F, Kyser K (2012) Isotopic composition of the elements In Isotopic Analysis: Fundamentals and applications using ICP-MS (1stedn), Edited by Vanhaecke F, Degryse P. Wiley-VCH GmbH & Co. KGaA, Weinheim.

[42] Trivedi MK, Branton A, Trivedi D, Nayak G, Panda P, Jana S (2016) Determination of isotopic abundance of $^{13}C/^{12}C$ or $^{2}H/^{1}H$ and $^{18}O/^{16}O$ in biofield energy treated 1-chloro-3-nitrobenzene (3-CNB) using gas chromatography-mass spectrometry. Science Journal of Analytical Chemistry 4: 42-51.

[43] Smith RM (2004) Understanding Mass Spectra: A Basic Approach, Second Edition, John Wiley & Sons, Inc, ISBN 0-471-42949-X.

[44] Meija J, Coplen TB, Berglund M, Brand WA, De Bievre P, Groning M, Holden NE, Irrgeher J, Loss RD, Walczyk T, Prohaska T (2016) Isotopic compositions of the elements 2013 (IUPAC technical Report). Pure Appl Chem 88: 293-306.

[45] Asperger S (2003) Chemical Kinetics and Inorganic Reaction Mechanisms Springer science + Business media, New York.

[46] Trivedi MK, Mohan TRR (2016) Biofield energy signals, energy transmission and neutrinos. American Journal of Modern Physics 5: 172-176.

[47] Trivedi MK, Branton A, Trivedi D, Nayak G, Panda P, Jana S (2016) Mass spectrometric analysis of isotopic abundance ratio in biofield energy treated thymol. Frontiers in Applied Chemistry 1: 1-8.

[48] Cleland WW (2003) The use of isotope effects to determine enzyme mechanisms. J Biol Chem 278: 51975-51984.

[49] Nikolic VD, Illic DP, Nikolic LB, Stanojevic LP, Cakic MD, Tacic AD, Ilic-Stojanovic SS (2014) The synthesis and characterization of iron (II) gluconate. Advanced Technologies 3: 16-24.